Modelling and Simulation of a Single Particle in Laminar Flow Regime of a Newtonian Liquid

Jamnani Dinesh,[1]
[1]Alpha Project Services, Vadodara, Gujarat, India
Email: djamnani@hotmail.com
Phone: +91-9727222287

1 Abstract

The interaction of a single particle in straight rectangular channel in laminar flow is modelled explicitly using the set of Navier Stokes equation for the fluid motion and Newton momentum equation for the particle motion in Cartesian coordinate system. The evaluation of integral force acting on the particle along with the behaviour of streamlines as a function of Reynolds number Re_P < 120 is done in 2-D numerical simulation. An example of linear shear flow condition in rectangular channel is studied to investigate the nature of drag and lift force in 2 - D simulation and the kinematics of a single particle explicitly in 3-D simulation. The aim of the kinematics study is to evaluate the steady state position of this single particle kept in a fluid stream under the gravitational force. The 3-D simulation schemes for particulate flows are only presented here since the results generation takes long time for CPU speed limitation.

2 Introduction

The science relating the motion of a particle in Newtonian fluid is applied to the mechanism of controlling the path, direction, position, velocity or physical behaviour of particles. It plays a crucial role in chemical and biochemical engineering because of its numerous physical realization e.g. sedimentation, fluidization of solid suspension, lubricated transport, hydraulic fracturing of reservoir, slurries, etc.

In the current work, the consideration has been done of numerical modelling of the directing the position of a single particle in a laminar liquid. The position or the path of a single particle in the Newtonian fluid is controlled by the effect of forces acting on it. The set of equation describing the interaction of a single particle in straight rectangular channel with the laminar liquid is modelled explicitly using Cartesian coordinate system forming the Navier Stokes equation for the fluid motion and Newton momentum equation for the particle motion. The set of interacting explicit equations after transformation into non-dimensional form are implemented into CFD code using the boundary condition corresponding to the type of the flow condition viz. plug flow, shear flow and Poiseuille flow.

A special case of a particle prevented from free rotation in linear shear flow is studied where besides the analyses of drag coefficient; lift coefficient is plotted as a function of Reynolds number Re_P and is compared with other types of flow conditions in section ξ-3 simulation results.

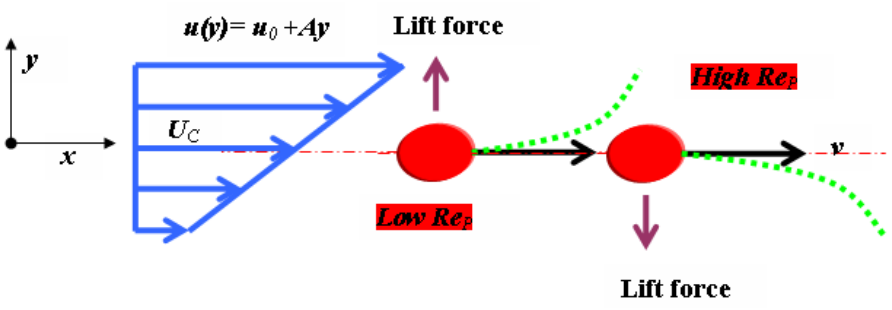

Figure 1: Schematics of a particle in linear shear flow.

As shown in figure 1 a single particle is kept in the middle of a rectangular channel having uniform shear flow. In shear flow a particle experience a transverse force (or lift force) which plays an important part in many practical situations to predict the lateral migration of particle.

The behaviour of drag coefficient, lift coefficient and wake formation are analysed as function of the Reynolds Re_P and shear parameter K to see the effects of varying velocity gradient on the force field around the particle.

After the assessment of the integral forces in 2-D simulation, the computation of integral forces around the particle in 3-D is done together with the additional volumetric force e.g. gravity force. These forces are used to determine the position and velocity vector of particle placed in the horizontal channel under the gravitational force acting in direction opposite to the fluid motion.

The time dependent flow is simulated where the particle position and velocity values computed from the force balance are fed back to the fluid motion equation and this iteration loop is continued until the steady position of the particle is attained. The steady state velocity of particle obtained is assessed against the terminal velocity of a particle. All the simulation results are documented together with the required figures and tables for easy understanding.

The main idea of this work is to maintain the position of particle in the fluid stream and evaluating the steady value of particle, its path and forces acting around it. The case of planar shear flow is taken as case study. For this the steady value of particle velocity is calculated from both stationary simulation and time dependent simulation. In both the simulation, the steady state value of particle velocity is study for different density ratio (0.5-3.0) of particle to the fluid. Finally the time dependent particle trajectory in the fluid stream of shear flow condition is plotted.

The model accompanied with transformation into non-dimensional form and the computation of the forces is discussed in section 3, implementation of model into CFD code and simulation scheme for 2-D and 3-D in section 4 and lastly simulation results are documented and shown graphically to discuss the relevant effect of the modelling and simulation in section 5.

3 Problem Definition

In modelling section the equation describing the physical model used in the current work is derived and discussed. The equations of fluid, particle motion equation followed by the integral force which couple both these equation are discussed. Finally before the implementation of the model it is transformed to non-dimensional form.

3.1 Basic equation and formulation for Newtonian Fluids (NS Equation)

The equation for the motion of an incompressible Newtonian liquid is described by the Navier-Stokes and the continuity equation (Patankar et al. 2000).

Navier-Stokes equation:

$$\rho_f\left(\frac{\partial u}{\partial t}+u\cdot\nabla u\right)-\nabla\cdot\sigma=b \qquad \text{in } \Omega f \text{ for } t\in[0,T] \qquad (1)$$

Continuity

$$\nabla\cdot u=0 \qquad \text{in } \Omega_f \text{ for } t\in[0,T] \qquad (2)$$

equation:

Total stress tensor:

$$\sigma = -pI + \mu_f \left[\nabla u + (\nabla u)^T\right] \quad (3)$$

Here u is the fluid velocity, ρ_f the fluid density, b is the body force or volumetric force, Ω_f is the domain occupied by the fluid at time t, I is the identity tensor, ∇ Napla operator, ∇^2 Laplace operator, μf the viscosity, p is the pressure and σ is the total stress tensor of the Newtonian fluid which consist of pressure stress and viscous stress. The integration of σ around the particle gives the value of forces acting on it. The modified Navier-Stokes equation for a Newtonian fluid consisting of pressure and viscous stress term after combining equation (1) and (3) is given below.

$$\rho_f \left(\frac{\partial u}{\partial t} + u \cdot \nabla u\right) = \rho_f g - \nabla p + \mu_f \nabla^2 u \qquad \text{in } \Omega_f \text{ for } t \in [0,T] \quad (4)$$

3.2 Equation of particle motion

A small rigid spherical particle of diameter d and radius r is considered to be located at a position $x(t)$ in a fluid. Its motion in the fluid stream is given by the well known Newton momentum equation neglecting its rotational motion and Magnus effect.

Newton's momentum equation:

$$m\frac{dv}{dt} = F \quad (5)$$

Resultant force vector:

$$F = (-1)\int_S \sigma.ndS \quad (6)$$

Position vector:

$$\frac{dX(t)}{dt} = v \quad (7)$$

Here, v is the particle velocity, m the mass of particle, $\partial\Omega p$ the boundary of the particle, n is the unit normal vector on the boundary $\partial\Omega$p pointing outward of the flow region, S is the outer boundary of particle and F is the resultant force (inertial force and viscous force) acting on the particle. Combining equation (5) and (6) the equation for the particle motion in the fluid flow is given as

Particle motion equation:

$$m\frac{dv}{dt} = \int_S \sigma.ndS \quad (8)$$

The interaction of an incompressible fluid and rigid particle belongs to the class of fluid-structure interaction problems. The coupling between the fluids specified by the equation (4) and a particle can be twofold, i.e. one-way or two-way. The coupling is one-way if a small particle is kept inside the fluid flow where there is no effect of a particle on the fluid motion. The other way around is also possible in some cases. The problem become more complicated if the motion of the particle is induced by the fluid flow and at the same time the fluid flow pattern is influenced by the particle motion. In the present work two-way coupling is considered since the particle is not large to neglect its influence.

Equation (4) and (7) are coupled to get two-way coupling interaction where the surface integration term in equation (7) is calculated from the Navier-Stokes equation (4) by evaluating the fluid stress tensor on the surface of the particle. The trajectory of the particle in the fluid stream is obtained by the iteratively solving the coupled Navier Stokes and particle motion equation. In that case first the Navier Stokes equation is solved using CFD software and the total stress tensor or the pressure and the viscous force acting on the particle is evaluated by integrating over the particle's surface. From this force the acceleration, velocity and particle position of the particle given by Newton's momentum equation (9) is calculated.

Acceleration of particle:

$$a = \frac{F}{m} = \frac{dv}{dt} \quad (9)$$

Velocity of particle:

$$v(t) = \int \left(\frac{F}{m}\right) dt \quad (10)$$

Solution of the integral equation (10) is given by analytical method as in equation (12) rather than relatively time consuming and inaccurate numerical method. Taking the initial condition for particle velocity as stationary and at located at position vector $x(t_0)$ or x_0 with velocity v0.

Initial condition of particle:

$$\text{Time } t = 0 \rightarrow x = x_0, \;\; v = v_0 \quad (11)$$

Velocity vector of particle:

$$v(t) = \int \left(\frac{F}{m}\right) dt \quad (12)$$

Position vector:

$$x(t) = \left(\frac{F}{m}\right) t^2 + v_0 t + x_0 \quad (13)$$

3.3 Computation of the forces

The force acting on the particle is usually the force arise due to the variation of the pressure forces and viscous forces on the particle surface. It can also be expressed in terms of the momentum flux far from the particle which does not require the knowledge of the flow in the vicinity of the particle (Batchelor 1970). Thus the forces acting on the particle in fluid flow are computed in two ways as described below:

1. Integration of the liquid stresses along the particle contour i.e. integration of forces acting in the vicinity of the particle.
2. Integration of all the forces and stresses along the boundaries of the computation domain i.e. forces on the body in terms of the momentum flux far from the body which does not require knowledge of the flow in the vicinity of the body.

The equalities of these two methods are verified in section 3: simulation results. The force acting around the particle in fluid consists of two parts: Surface force and Body force

Surface force = Pressure force + Viscous force (14)

Body force/ Volume force = Gravity force and Buoyancy force (15)

Alternatively the force acting on the single particle immersed in a fluid stream is represented by the lift force and drag force. The combined pressure and viscous force which acts in opposite to the direction of fluid stream is termed as drag force whereas in direction perpendicular to the drag force is termed as lift force. The drag force is the resistance force to the motion of an immersed particle imparts by the fluid and hence it determines the velocity and acceleration of the particle. The values of drag force in the form of drag coefficient are compared as the benchmark test and are used in evaluating the effect of the CFD coding in determination of the integral force.

The lift force consists of the buoyancy force and gravitational force in case of horizontal flow. It determines the motion of the particle perpendicular to the fluid motion and is important factor in a shear flow condition. For 2D fluid flow, the drag force and the lift force are given by the equation (15) and (16) respectively:

$$F_D = \int_S \left(\rho_f \mu_f \frac{\partial u}{\partial n} n_y - p n_x \right) dS \qquad (16)$$

Drag force = Viscous term + Pressure term (in x-direction)

$$F_L = \int_S \left(\rho_f \mu_f \frac{\partial u}{\partial n} n_x + p n_y \right) dS \qquad (17)$$

Lift force = Viscous term – Pressure term (in y-direction)

Alternatively, Lift force = Gravity force(↓) + Buoyancy force(↑)

Pictorially the forces acting around the particle in the fluid stream is presented as shown in Figure . In current situation the lift force is the resultant force acting in the y-direction and the drag in the x-direction. The pressure force acting on the particle is the resultant of the inertial effect of the fluid and viscous force as the resultant of the viscous effect of the fluid.

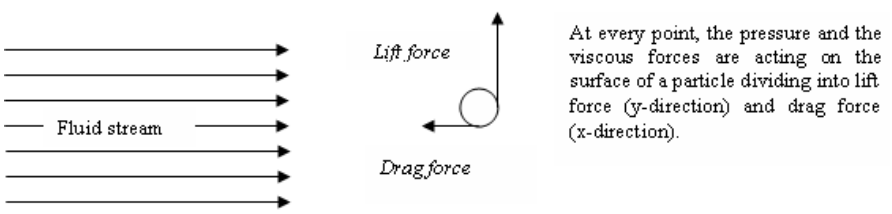

Figure 2: Pictorially representation of forces around the particle

The expression for drag force and lift coefficient in terms of drag force and lift force for 2-D particulate flow are given below (Turek et al.).

Drag coefficient: $C_D = \frac{2F_D}{\rho_F u^2 d}$ Lift coefficient: $C_L = \frac{2F_L}{\rho_F u^2 d}$ (17)

3.4 Transformation into non-dimensional form (Scaling)

Scaling the variables in the Navier-Stokes and the particle motion equations transformed these equations into non-dimensional form which is useful to improve the solution of the coupled equation. Consider U_C, i.e. free stream fluid velocity, as a characteristic velocity and d, diameter of particle as the characteristic length; the dimensionless variables are given in equation (19).

$$U = \frac{u}{U_C} \qquad V = \frac{v}{U_C} \qquad P = \frac{p}{\rho_f U_C^{\,2}}$$
$$\bar{t} = \frac{t U_C}{d} \qquad \bar{\nabla} = d\nabla \qquad \bar{\nabla}^2 = d^2 \nabla^2 \qquad (19)$$

The non-dimensional form of Navier-Stokes, continuity and Newton equations after scaling is given below.

Navier-Stokes:
$$\left(\frac{\partial U}{\partial \bar{t}} + U \cdot \bar{\nabla} U \right) = -\bar{\nabla} \cdot P + \frac{1}{\mathrm{Re}} \bar{\nabla}^2 \cdot U - G \qquad (9)$$

Continuity equation:
$$\bar{\nabla} \cdot U = 0 \qquad (10)$$

Newton's momentum equation:
$$\frac{m}{\rho_f d^3} \mathrm{Re}_P \left(\frac{dV}{d\bar{t}} - g \right) = \bar{F} \qquad (11)$$

Here, U, V, P, $\bar{t}$, $\bar{\nabla}$, $\bar{\nabla}^2$ are the dimensionless fluid velocity, particle velocity, pressure, time, Del operator and Laplace operator. m is the mass of a particle, Re_P is the Reynolds number based on a particle's diameter and G is the dimensionless gravity number and $\bar{F}$ is the dimensionless resultant force acting on the particle.

$$\mathrm{Re}_p = \frac{U_0 \rho_f d}{\mu_f} \qquad G = \frac{\rho_f g d^2}{\mu_f} \qquad \bar{F} = \frac{F}{\mu_f U_0 d} \qquad (12)$$

In dimensionless form C_D and C_L becomes twice the force equivalent and are given below where $\overline{C_D}$ and $\overline{C_L}$ are dimensionless coefficient.

Drag coefficient: $\overline{C_D} = \overline{F_D}$ *Lift coefficient:* $\overline{C_L} = \overline{F_L}$ (18)

The equation of motion of particle in non-dimensional form is solved by applying the time step of 5/100 (where 5 = width of the channel, 100 = step change).

4 Use of Comsol Multiphysic

The complete model is implemented in Comsol 3.1 (FEMLAB). Since Comsol 3.1 is a stand alone CFD package where it is not feasible to simulate the model in loop required for data manipulation and controlling steps. MATLAB's m-file programming interface is used to assist in controlling the FEMLAB simulation.

First the assessment of the data computed is done for 2-D static incompressible flow past a long cylinder placed in a straight channel at right angle to the incoming fluid as shown in *Figure* 3. The cylinder is kept in the centre to have the steady-state symmetrical flow.

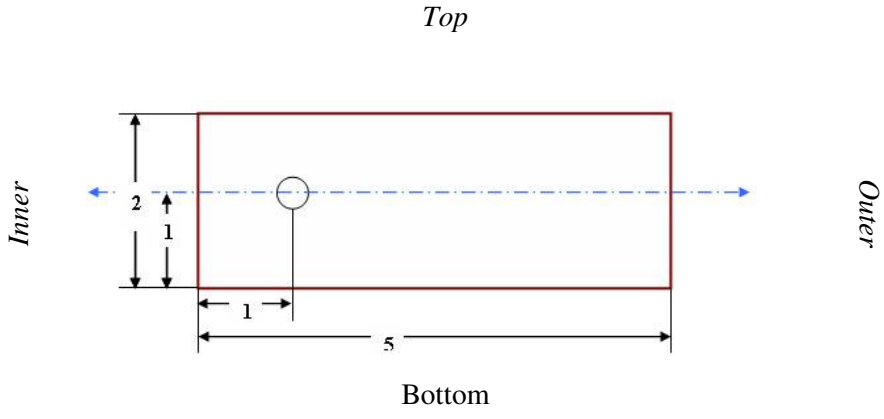

Figure 3: Boundary condition and sub-domain section for 2-D modelling and simulation results

The computation of Drag force (F_D) and Lift force (F_L) acting on the cylinder can be done from the gradient of velocity field and the pressure field on the cylinder's surface by taking the differentiation of FEMLAB solution value on its surface. But more efficient and time saving way of doing it is to use pair of weak constraint variable which is second order polynomial of the viscous and pressure force fields. This is done by integrating boundary of the particle surface by weak constraint. In the subsequent section the parameter selection and reason for particular choice is explained in detailed.

Table 1:Mesh parameter used in simulation

	2-D Model	3-D Model
Predefined mesh size	Normal	Normal
Maximum element size scaling factor	0.3	1
Element growth rate	1.2	1.4
Mesh curve factor	0.25	0.4
Mesh curvature cut off	0.0003	0.001
Mesh geometry to level	Sub-domain	Sub-domain
Number of elements	5262	16475
Number of boundary elements	168	1850
Minimum element quality	0.5068	0.3329
Degree of freedom	Around 24,000	Around 85,000
Number of edge elements	-	140

Both unstructured or block structured give the same results and hence either one of them is used which work automatically in Comsol through mesh mapping.

4.1 Computational scheme

The types of 2D and 3D modelling and their simulation steps performed in programming are shown in flow chart or algorithm steps.

The main aim of 2D modelling is to validate the forces around the circle in the fluid flow as shown in *Figure* 5. In 3D modelling stationary simulation to calculate the steady state particle velocity and the particle trajectory is determined.

4.1.1 2D flow-stationary simulation

The following steps are employed in solving the 2D modelling of infinite length cylinder in the fluid stream:

1. First the geometry of a rectangular channel of length L = 5 unit and width W = 2 unit with circle of diameter positioning in the centre of the channel having coordinate (x, y) = (1, 1) is made.
2. Set the value of Re_P through MATLAB m-file interface.
3. Set the physical properties of a fluid stream viz. density ρf =1 and viscosity $\mu f = 1/ ReP$ according to the non-dimensional form of Navier Stoke equation (9)
4. Select the outer boundary of the channel as per the type of flow condition selected e.g. plug flow, shear flow or Poiseuille flow. Boundary condition of circle is selected as 'no slip' condition.
5. Refined the mesh near the circle-fluid interface in order to improve convergence and better the value of the solution.
6. Select weak non-ideal weak constraint mode as Lagrange multiplier element over the entire domain to calculate the integral forces on the boundary of circular cylinder rather than rather than
7. Set non-ideal weak mode of constraint under the option properties of physics menu.
8. Compute the drag and lift force in the post-processing mode by integration of boundary of circle.

Steps from 1 to 5 are then repeated through MATLAB m-file interface with FEMLAB by changing the Re values given that the simulation continues.

Finally the plot of drag coefficient and lift coefficient against Reynolds number (Re) was plotted and explained in simulation results section.

4.1.2 3D flow-stationary and unsteady state simulation

3-D simulation is performed on the horizontal rectangular section imitating the vertical channel where the flow is against the gravitational force. It is discuss only for shear flow condition evaluating the stationary and the unsteady state simulation variables.

In stationary shear flow calculation the particle is fixed on its placed and the balanced position of the particle is obtained by changing its density with respect to the fluid density against varying the flow-rate in terms of Reynolds number Re_P.

In time dependent simulation of the shear flow condition, the terminal velocity of the particle suspended is calculated. This is done by computing the velocity vector and the position vector of a particle from the integral forces and substituting again the velocity of particle back to the 3-D simulation of the fluid motion with particle using equation (9) and (11) on each time step (t_S). The time step is taken as 5/100, where 5 is the residence time for the fluid flowing at the rate of 1 unit/sec.

Stationary and unsteady state 3D calculations of particle velocity in shear flow were performed by two algorithms given below

1. Calculation of the steady state relation between the density ratio and the Re_P balancing all the integral forces acting on a particle.
2. Time-dependent particle position computed from the integrated fluid forces around the particle

The steps for implementing the 3D modelling is same as 2D except the inclusion of the gravity force opposite to that of drag force and the controlling of particle motion according to the flow chart.

Stationary simulation steps

The following steps are used in stationary simulation as also described below:

1. Select incompressible Navier-Stokes model in 3-D solver and apply non-dimensional form of equation (10) as the fluid modelling equation.
2. Set up the Re_P to the laminar flow regime ($10^0 < Re_P < 10^2$).
3. Substitute the value of density $\rho f = 1$ and viscosity $\mu_f = 1/Re_P$
4. Select 'no slip' condition for the boundary of a circle interacting with the fluid.
5. Apply dimensionless gravitational force using equation (12) against the direction the direction of the flow to imitate it as the vertical upward motion of a fluid upon the particle against the gravity.
6. Mesh the geometry with finer mesh area near the particles surface.
7. Run the simulation with the non-linear GMRES solver with weak mode of constraint. i.e. weak condition apply to the boundary of the particle.
8. Compute all the integral forces around the particle acting in x, y and z-direction. Theses forces are then substituted to obtained the particle position vector and the particle velocity vector.
9. Construct a plot of density ratio against velocity vector for different Re_P.
10. The minimum point of the curve is the required point where the density of a particle is small enough to balance the gravity force and the convective force acting of the fluid.

Unsteady state simulation steps

Following are the steps that were used in stationary simulation as also described by flow chart (*Figure* 7):

1. First set the velocity of fluid as obtained in stationary simulation and compute the corresponding *ReP*.
2. Positioned the particle in the middle of the rectangular channel with initial velocity of zero magnitude in all the direction i.e. V = (0,0,0).
3. Perform the same steps 1, 3, 5, 6, 7 steps of stationary simulation steps.
4. Compute the integral forces around the particle in x, y and z direction. The forces $\overline{F_X}$, $\overline{F_Y}$ and $\overline{F_Z}$ computed are non-dimensional forces and then drag, lift and suction coefficient. From the value of this coefficient, calculate the velocity vector $\overline{V}$ of particle using equation (20) taking time steps of 5/10. (Where 5 = length of channel and U = 1 m/s is non-dimensional velocity of fluid stream and 10 = time step).
5. Calculate the x-position of particle by using equation (23). Similarly calculate the y- and z- position of particle.
6. Update the position and velocity of a particle found from the integral forces.

7. Check the magnitude of particle velocity in x-direction. If it is around '1' then the particle is moving with the same velocity as the fluid under the effect of gravitational force.
8. Repeat steps from 1 to 7 until converge obtained.

At each time step, the previous flow field gives the forces on the particle, whose motion is then explicitly updated by Newton's law, giving rise to a new domain. After re-meshing and mapping the old flow field onto the new mesh, the nonlinear Navier Stokes equations are solved by FEMLAB which are part of the boundary conditions for the fluid flow and then iteratively with the Newton's equation of particle velocities.

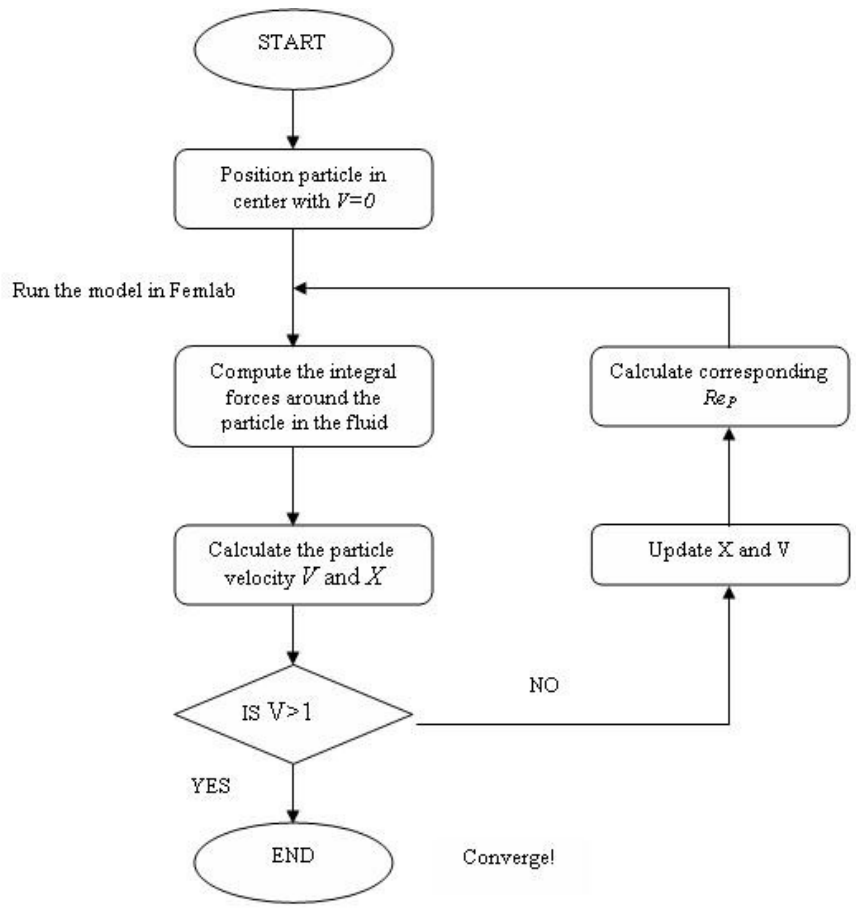

Figure 4: Flow chart for unsteady state simulation of particle motion in fluid

5 Simulation Results

For the 2D simulation results are analysed, where the drag coefficient CD of a circle in a straight channel with different boundary conditions are compared and investigated. The behaviour in the wake of the cylinder is examined and presented pictorially. The case study of a shear flow is then considered, where besides the drag coefficient, the lift coefficient CL has also been analysed.

For 3D problem simulation results are unable to generate and are kept for future work.

5.1 Two dimensional simulation results

This is the benchmark test for the hydrodynamic forces computed around the single particle in fluid flow. The results obtained give the insight into the efficiency of the Comsol Software.

A circle of diameter 0.1 units is placed in the centre of the rectangular channel of length 5 units and width 2 units. The equivalence of particle in the 3D fluid flow is taken as a circle in the straight channel which can be viewed as cylinder of infinite length in 3D dimension space. The boundary condition varies depending on the type of the flow needed to be simulated. There are 5 different types of planar flow conditions which are simulated and documented.

1. Plug flow with homogenous boundary condition and incompressible Navier stokes model.
2. Plug flow with neutral boundary condition and incompressible Navier stokes model.
3. Plug flow with homogenous boundary condition and k-ε turbulent model.
4. Shear flow condition with incompressible Navier stokes model.
5. Poiseuille flow condition with incompressible Navier stokes model.

The values of drag coefficient in all these 5 flow conditions are compared with the experimental values of the flow past the cylinder and its deviation from the experimental values in regards to the flow conditions is explained along with the behaviour of the streamlines behind the cylinder or circle in the channel.

5.1.1 Computation of the forces by two methods

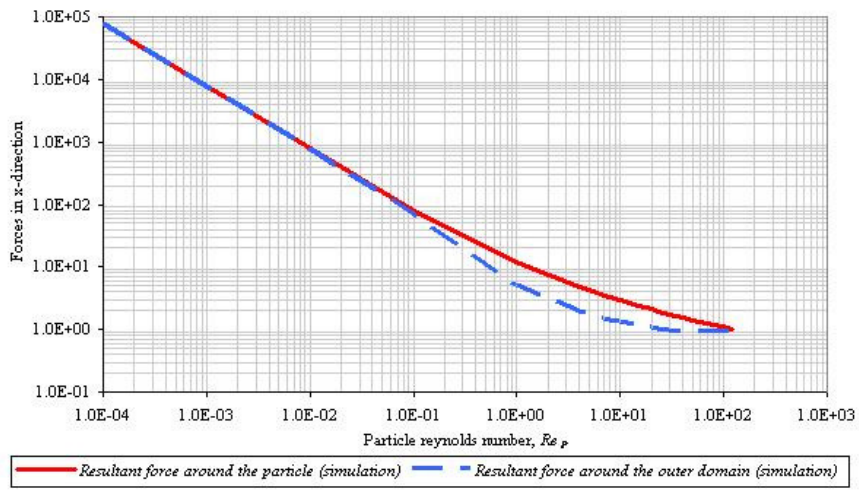

Figure 5: Comparison of 2-D simulated x-directional forces

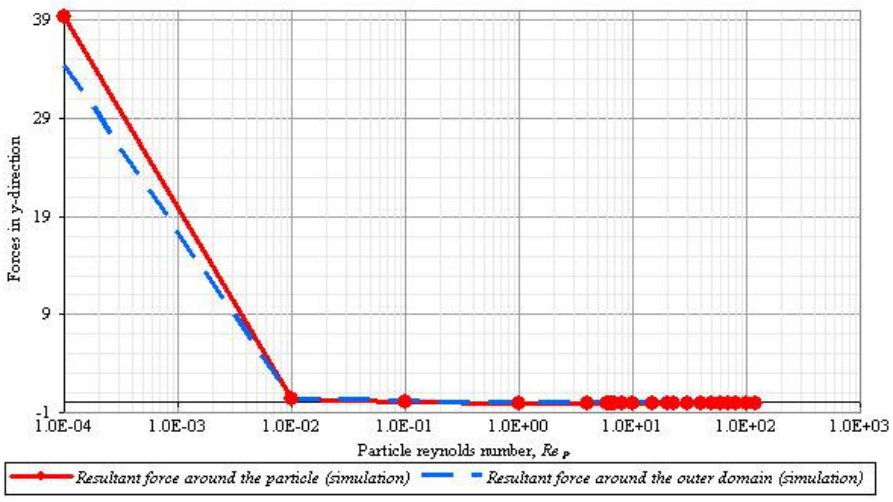

Figure 6: Comparison of 2-D simulated y-directional forces

Comparing the force acting in x-direction around the particle and around the outer domain as shown in figure 5, there is slight deviation between the forces at high particle Reynolds number $0.1 < Re_P < 100$ whereas in case of y-direction figure 6 it is in low particle Reynolds number $Re_P > 0.1$. This slight deviation can be ignored since at high Re_P the value of x-direction forces are low.

5.1.2 Review of drag coefficient and Behaviour of streamline

The drag coefficient values calculated in each of these five flow condition have been plotted as a function of particle Reynolds number Re_P and compared with standard values given by Sucker and Brauer (1975). The values of drag coefficient with Re_P for all the flow condition are tabulated in Appendix-A Section 7.

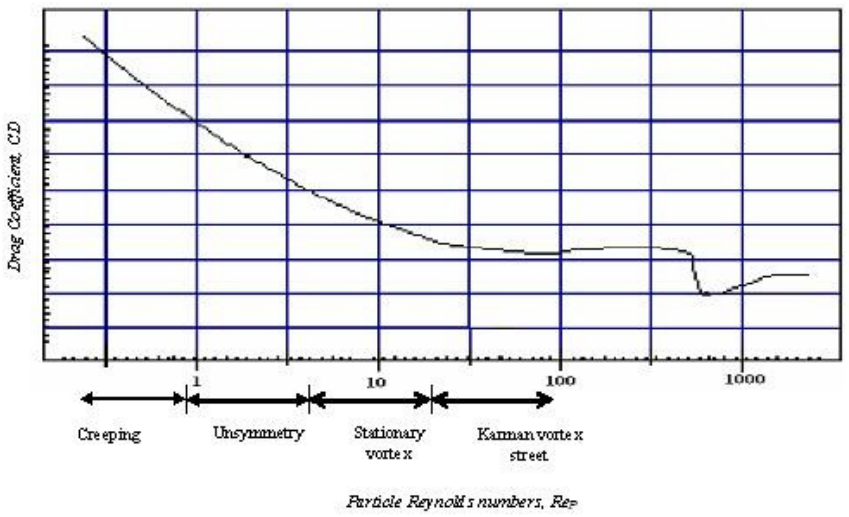

Figure 7: Experimental results for drag coefficients, its viscous and pressure term against Reynolds number
(Source: Schlichting et al. 1996)

There are several different regions observed during motion of particle in the fluid stream during laminar flow condition as differentiated in the plot of drag coefficient C_D against Reynolds number Re_P figure 7. The corresponding streamline behaviour is provided by Schlichting et al. (1996) along with the range of C_D values as shown in figure 8.

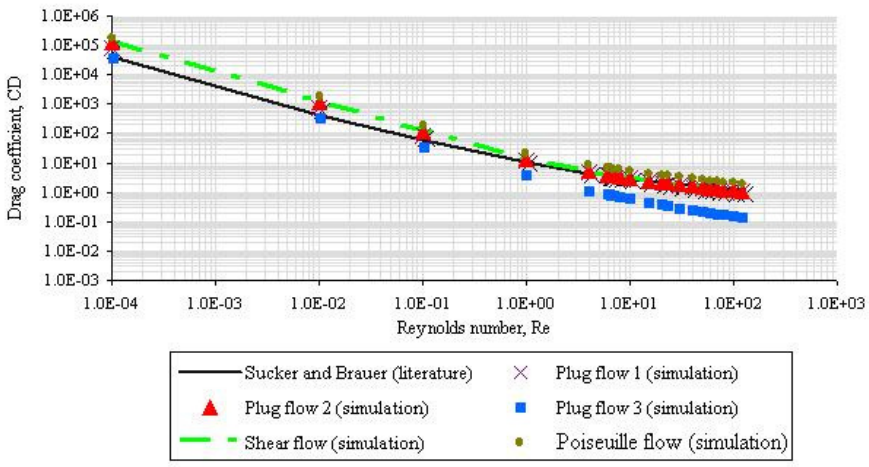

Figure 6: Log-log plot of C_D against Re_P for different flow conditions

5.1.3 Assessment of lift force in Shear flow condition

The Shear flow is characterized by the linear velocity field of fluid is explained in appendix A. At the top end boundary the fluid is moving with maximum velocity *umax* and at the bottom with zero velocity or 'no slip' condition. It is found that curve of Re_P against C_D of shear flow is same as plug flow with neutral boundary condition.

In shear flow besides drag, a lift force is also important factor in deciding the direction of the particle. Due to the nature of shear flow the forces around the particle perpendicular to the flow have some non-zero value which can't be neglected in the determination of the particle trajectory.

The lift coefficient or so called dimensionless lift force obtained by the current simulation results has been plotted as a function of particle Reynolds number Re_P and compared the same with calculated lift force in plug flow and Poiseuille flow. The values of lift coefficient C_L are calculated for different Reynolds number by changing it instead of changing the flow velocity which is dimensionless velocity in the model equation.

The lift force as shown in figure 10 is almost zero in un-sheared flow. This is due to the uniform flow pattern and one dimension velocity field in plug flow and Poiseuille flow. It can be non-zero at particle Reynolds number $Re_P < 300$ as observed by Kurose and Komori (1999). The values of lift coefficient in shear flow are found to be constant at high Re_P which is in agreement with the Saffman (1965). The unexpected behaviour of C_L i.e. shifting of values from positive to negative and back to positive at particular Re_P cannot be explained in the context of the theoretical investigation.

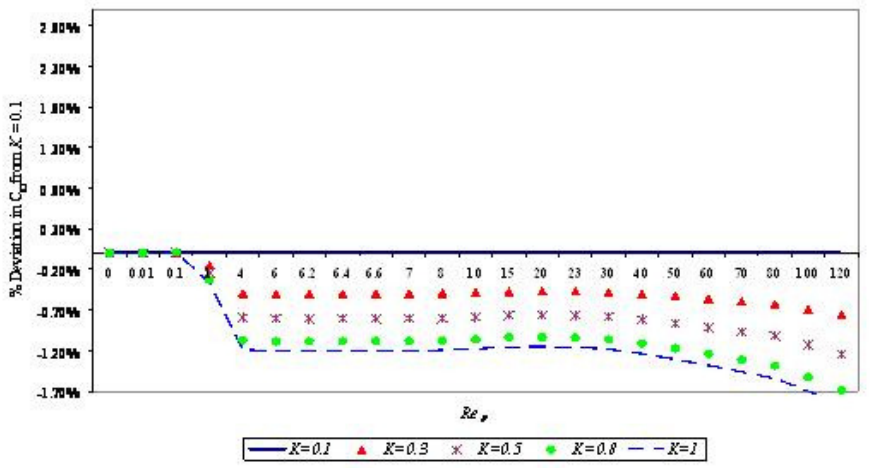

Figure 9: Plot showing % deviation in the drag coefficient among shear flow having varying shear parameter

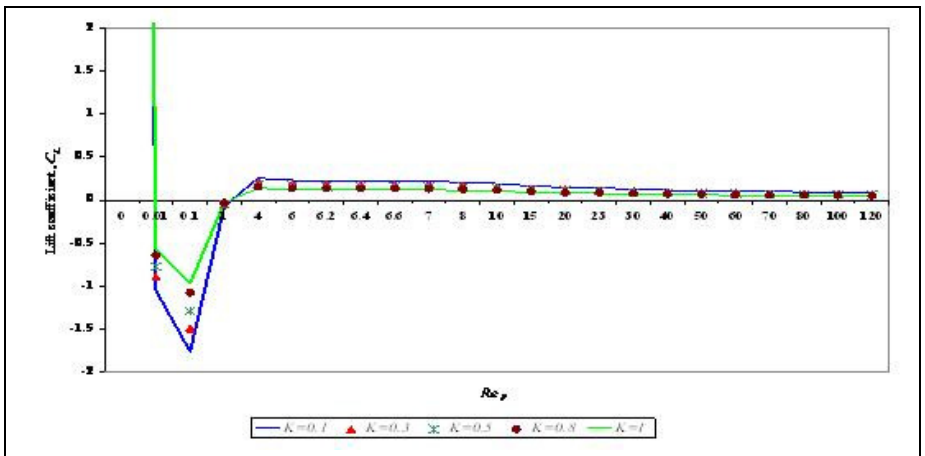

Figure 10: Plot of lift coefficient as a function of Reynolds number for different shear parameter K

The behaviour of streamline as also explained in the introduction section is different from the plug flow and Poiseuille flow. The length of the vortex is proportional to the drag coefficient as already noted, there is onset of Karman vortex formation in shear flow at around $Re_P = 50$ which is not visible in uniform flow. This streamline nature is different from the plug flow whose pattern of C_D against Re_P plot is same as that of the shear flow. In shear flow the streamline seems to be having re-circulating zone pointing downward. This can be due to attraction of particle to the lower end having low velocity profile at high Re_P as also explained by Feng and Josep (1995). The influence of the dimensionless shear rate or shear parameter K cannot be neglected on the lift coefficient and therefore is considered in the next section.

Lift coefficient with varying shear parameter

The plot of drag coefficient in % difference as a function of Reynolds number for different K shows that at low Re_P higher the value of K lower is the C_D values Similarly the plot of C_L against Re_P shows that the higher the value of K higher is the C_L values at low Reynolds number. Both these characteristic of the 2-D shear flow condition is in accordance with the investigation made by Kang (2006).

6 Conclusion

2-D Simulation results for the computation of integral forces around single particle obtained were in agreement with the experimental valves from literature study. The integral forces around particle around outer domain shows resemblance similarly the simulation results for Drag coefficient and Lift coefficient shows agreement at low Reynolds which can also attribute to the inefficiency of solver at high Reynolds number. For 3-D

simulation only flowchart showing simulation steps are discuss since simulation results are hard to generate owing to CPU limitation.

7 Appendix A

7.1 Appendix A1: Boundary conditions for plug, shear and Poiseuille flow

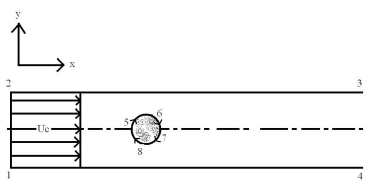

Plug flow

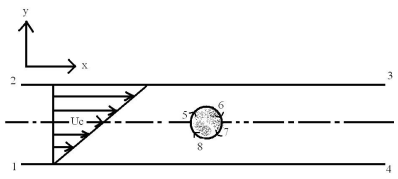

Shear flow with K = 1

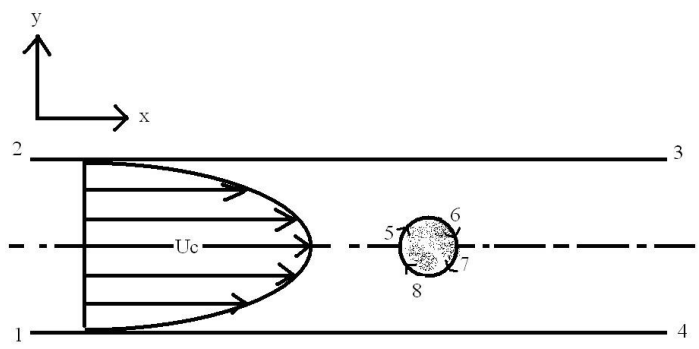

Poiseuille flow

Figure11:Schematic of a different flow condition with particle in centre showing vertex labels
(1-2: Inflow side; 2-3: Top side; 1-4: Bottom side; 3-4: Outflow side; 5-8: circle boundary, U_C = Approach velocity = 1 in all the flow conditions)

Plug flow with homogeneous boundary conditions Inflow side: Constant input velocity, *Ux=UC* Top and Bottom side: Constant input velocity field only in x-direction, *Ux=UC* Outflow side: Zero pressure Circle boundary: No slip condition	**Plug flow with neutral boundary conditions:** Inflow side: Constant input velocity, $Ux=U_C$ Top and Bottom side: Neutral boundary / no stress across the boundary Outflow side: Zero pressure Circle boundary: No slip condition
Shear flow Inflow side: Linear velocity profile with slope A (velocity gradient), $Ux=U_C*y*2$ Top side: Constant maximum velocity in x-direction Bottom side: Zero velocity , *Ux=0* Outflow side: Zero pressure Circle boundary: No slip condition	**Poiseuille flow** Inflow side: Parabolic velocity profile, *Ux=6*(1-y2)*UC* Top side and Bottom side: No slip condition Outflow side: Zero pressure **Circle boundary: No slip condition**

7.2 Appendix A2: 2D simulation results data

7.2.1 Plug flow

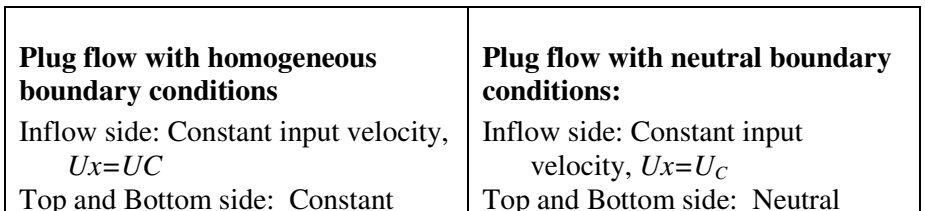

Figure 12: Schematic of observed wake behaviour behind the circle in 2-D plug flow in the simulation results

7.2.2 Shear flow

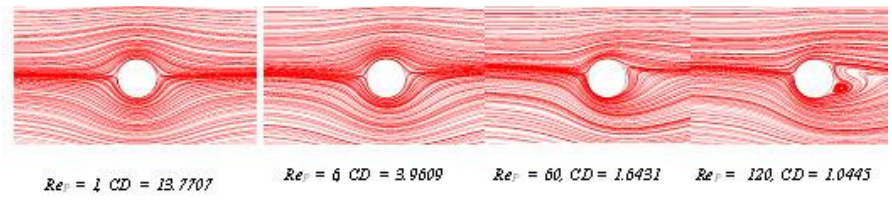

Figure 13: Schematic of observed wake behaviour behind the circle in 2-D shear flow in the simulation results

7.2.3 Poiseuille flow

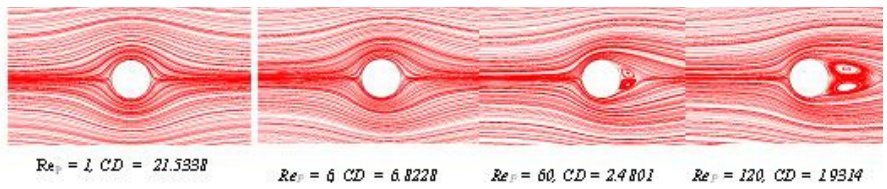

Figure 14: Schematic of observed wake behaviour behind the circle in 2-D Poiseuille flow in the simulation results

7.3 Appendix A3: Plot of pressure force and viscous force for different flow condition

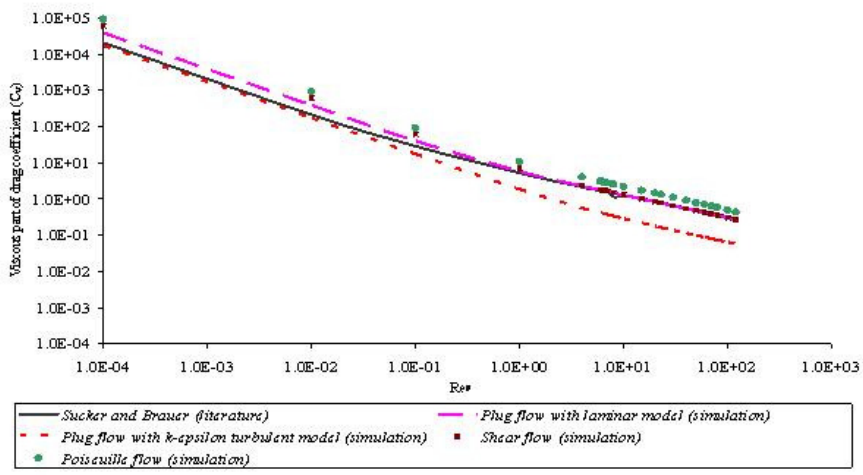

Figure 15: Log-log plot of viscous part of the drag coefficient for 2-D flow over circular cylinder: comparison between literature and simulation results

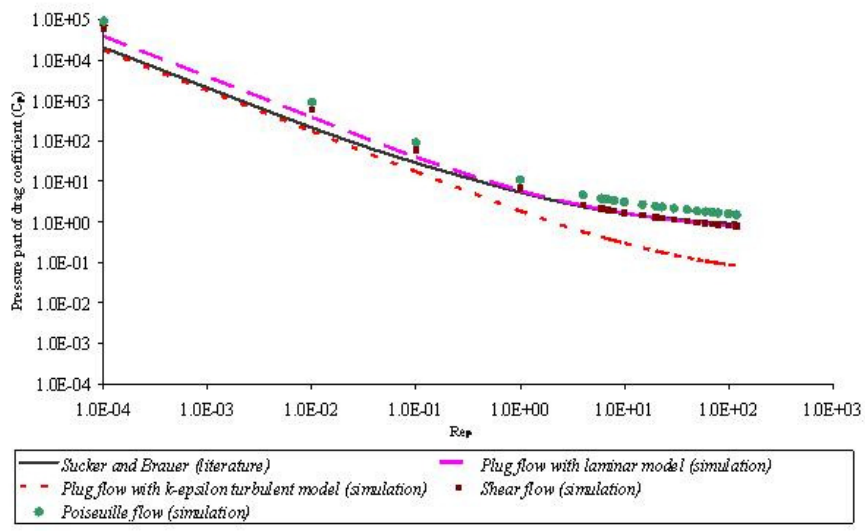

Figure 16: Log-log plot of pressure part of the drag coefficient for 2-D flow over circular cylinder: comparison between literature and simulation results

Table 2: Values of drag coefficient as a function of Reynolds number for different flow con

Particle Reynolds number, Re_P	Sucker and Brauer (literature)	Plug Flow 1 (simulation)	Plug Flow 2 (simulation)	Plug flow 1 with k-epsilon turbulent model (simulation)	Shear flow (simulation)	Poiseuille (simulatio
0.0001	40560.00	77096.92	121156.0272	34426.6849	121156.0321	18150
0.01	424.7000	773.1255	1211.5866	344.5152	1211.5888	1815
0.1	57.2370	79.7992	121.4179	34.6783	121.4489	182.
1	10.5800	11.6638	13.8596	3.7024	13.7707	21.533
4	4.5020	4.7953	5.1504	1.1271	5.0463	8.5280
6	3.6510	3.8137	4.0439	0.8336	3.9609	6.8225
6.2	3.5880	3.7461	3.9688	0.8141	3.8874	6.7055
6.4	3.5280	3.6822	3.8978	0.7958	3.8179	6.5948
6.6	3.4660	3.6215	3.8306	0.7786	3.7521	6.4899
7	3.3650	3.5090	3.7063	0.7468	3.6306	6.2954
8	2.8580	3.2703	3.4437	0.6800	3.3737	5.8827
10	2.8310	2.9168	3.0579	0.5832	2.9966	5.2714
15	2.4516	2.3943	2.4945	0.4447	2.4454	4.3653
20	2.1780	2.0978	2.1784	0.3694	2.1357	3.8475
23	2.0380	1.9717	2.0449	0.3385	2.0046	3.6259
30	1.8250	1.7592	1.8211	0.2880	1.7844	3.2495
40	1.6330	1.5630	1.6160	0.2439	1.5820	2.8974
50	1.5200	1.4308	1.4787	0.2158	1.4459	2.6573

60	1.4350	1.3336	1.3785	0.1961	1.3461	2.4301
70	1.3710	1.2581	1.3011	0.1815	1.2689	2.3433
80	1.3210	1.1973	1.2391	0.1701	1.2068	2.2346
100	1.2420	1.1046	1.1453	0.1534	1.1126	2.0653
120	1.2040	1.0372	1.0780	0.1416	1.0445	1.9314

8 Appendix C: References

Aidun, C. K., Lu, Y. N., and Ding, E. J. (1998). "Direct analysis of particulate suspensions with inertia using the discrete Boltzmann equation." ***Journal of Fluid Mechanics*, 373, 287-311.**

Batchelo.Gk. (1970). "Stress System in a Suspension of Force-Free Particles." ***Journal of Fluid Mechanics*, 41, 545-&.**

Ben Richou, A., Ambari, A., and Naciri, J. K. (2004). "Drag force on a circular cylinder midway between two parallel plates at very low Reynolds numbers - Part 1: Poiseuille flow (numerical)." ***Chemical Engineering Science*, 59(15), 3215-3222**.

Borthwick, A. (1986). "Comparison between 2 Finite-Difference Schemes for Computing the Flow around a Cylinder." ***International Journal for Numerical Methods in Fluids*, 6(5), 275-290.**

Churchill, S. W. (1988). "Viscous Flows: The practical use of theory." 317-407.

Ding, E. J., and Aidun, C. K. (2000). "The dynamics and scaling law for particles suspended in shear flow with inertia." ***Journal of Fluid Mechanics*, 423, 317-344.**

Feng, J., Hu, H. H., and Joseph, D. D. (1994a). "Direct Simulation of Initial-Value Problems for the Motion of Solid Bodies in a Newtonian Fluid .1. Sedimentation." ***Journal of Fluid Mechanics*, 261, 95-134.**

Feng, J., Hu, H. H., and Joseph, D. D. (1994b). "Direct Simulation of Initial-Value Problems for the Motion of Solid Bodies in a Newtonian Fluid .2. Couette and Poiseuille Flows." ***Journal of Fluid Mechanics*, 277, 271-301.**

Feng, J., and Joseph, D. D. (1995). "The Unsteady Motion of Solid Bodies in Creeping Flows." ***Journal of Fluid Mechanics*, 303, 83-102.**

Gutfinger, C., Pnueli, D., Moldavsky, L., Shuster, K., and Fichman, M. (2003). "Particle motion in simple shear flow with gravity." ***Aerosol Science and Technology*, 37(10), 841-845.**

Howe, M. S. (1995). "On the Force and Moment on a Body in an Incompressible Fluid, with Application to Rigid Bodies and Bubbles at High and Low Reynolds-Numbers." *Quarterly* ***Journal of Mechanics and Applied Mathematics*, 48, 401-426.**

Jeffrey, R. C., and Pearson, J. R. A. (1965). "Particle Motion in Laminar Vertical Tube Flow." ***Journal of Fluid Mechanics*, 22, 721-&.**

Jordan, S. K., and Fromm, J. E. (1972). "Laminar-Flow Past a Circle in a Shear-Flow." ***Physics of Fluids*, 15(6), 972-&.**

Kang, S. (2006). "Uniform-shear flow over a circular cylinder at low Reynolds numbers." ***Journal of Fluids and Structures*, 22(4), 541-555.**

Karnis, A., Goldsmit.Hl, and Mason, S. G. (1966). "Flow of Suspensions through Tubes .V. Inertial Effects." ***Canadian Journal of Chemical Engineering*, 44(4), 181-&**.

Kiya, M., Tamura, H., and Arie, M. (1980). "Vortex Shedding from a Circular-Cylinder in Moderate-Reynolds-Number Shear-Flow." ***Journal of Fluid Mechanics*, 101(DEC), 721-&.**

Kurose, R., and Komori, S. (1999). "Drag and lift forces on a rotating sphere in a linear shear flow." ***Journal of Fluid Mechanics*, 384, 183-206.**

Kuzmin, D. (2006). "Computational Fluid dynamics."

Legendre, D., and Magnaudet, J. (1998). "The lift force on a spherical bubble in a viscous linear shear flow." ***Journal of Fluid Mechanics*, 368, 81-126.**

Lei, C., Cheng, L., Armfield, S. W., and Kavanagh, K. (2000). "Vortex shedding suppression for flow over a circular cylinder near a plane boundary." *Ocean Engineering*, 27(10), 1109-1127.

Maxey, M. R., and Riley, J. J. (1983). "Equation of Motion for a Small Rigid Sphere in a Nonuniform Flow." ***Physics of Fluids*, 26(4), 883-889.**

Mikulencak, D. R., and Morris, J. F. (2004). "Stationary shear flow around fixed and free bodies at finite Reynolds number." ***Journal of Fluid Mechanics*, 520, 215-242.**

Nakabayashi, K., Yoshida, N., and Aoi, T. (1993). "Numerical-Analysis for Viscous Shear Flows Past a Circular-Cylinder at Intermediate Reynolds-Numbers." ***JSME International Journal Series B-Fluids and Thermal Engineering*, 36(1), 34-41.**

Norberg, C. (2001). "Flow around a circular cylinder: Aspects of fluctuating lift." ***Journal of Fluids and Structures*, 15(3-4), 459-469.**

Pan, T. W. (1999). "Numerical simulation of the motion of a ball falling in an incompressible viscous fluid." ***Comptes Rendus De L Academie Des Sciences Serie Ii Fascicule B-Mecanique Physique Astronomie*, 327(10), 1035-1038.**

Patankar, N. A., Singh, P., Joseph, D. D., Glowinski, R., and Pan, T. W. (2000). "A new formulation of the distributed Lagrange multiplier/fictitious domain method for particulate flows." ***International Journal of Multiphase Flow*, 26(9), 1509-1524.**

Rajagopalan, S., and Antonia, R. A. (2005). "Flow around a circular cylinder - structure of the near wake shear layer." *Experiments in Fluids*, 38(4), 393-402.

Repetti, R. V., and Leonard, E. F. (1964). "Segre-Silberberg Annulus Formation - Possible Explanation." ***Nature*, 203(495), 1346-&**.

Saffman, P. G. (1965). "Lift on a Small Sphere in a Slow Shear Flow." ***Journal of Fluid Mechanics*, 22, 385-&.**

Schlichting, H., and Gersten, K. (1996). "Boundary layer Theory." 801.

Segre, G., and Silberberg, A. (1962). "Behaviour of Macroscopic Rigid Spheres in Poiseuille Flow .2. Experimental Results and Interpretation." ***Journal of Fluid Mechanics*, 14(1), 136-157.**

Sucker, D., and Brauer, H. (1975). "Investigation of Flow around Transverse Cylinders." ***Warme Und Stoffubertragung-Thermo and Fluid Dynamics*, 8(3), 149-158.**

Tritton, D. J. (1959). "Experiments on the Flow Past a Circular Cylinder at Low Reynolds Numbers." ***Journal of Fluid Mechanics*, 6(4), 547-&.**

Turek, S., Rannacher, R., and Schäfer, M. "Evaluation of a CFD benchmark for laminar flows."

Turek, S., and Wan, D. "Fictitious boundary and moving mesh methods for the numerical simulations of rigid particulate flows."

Vasseur, P., and Cox, R. G. (1976). "Lateral Migration of a Spherical-Particle in 2-Dimensional Shear Flows." ***Journal of Fluid Mechanics*, 78(NOV23), 385-413.**

Wen, C. Y., Yeh, C. L., Wang, M. J., and Lin, C. Y. (2004). "On the drag of two-dimensional flow about a circular cylinder." ***Physics of Fluids*, 16(10), 3828-3831.**

Williamson, C. H. K. (1996). "Vortex dynamics in the cylinder wake." ***Annual Review of Fluid Mechanics*, 28, 477-539.**

Wu, T., and Chen, C. F. (2000). "Laminar boundary-layer separation over a circular cylinder in uniform shear flow." ***Acta Mechanica*, 144(1-2), 71-82.**

Yang, B. H., Wang, J., Joseph, D. D., Hu, H. H., Pan, T. W., and Glowinsk, R. (2005). "Migration of a sphere in tube flow." ***Journal of Fluid Mechanics*, 540, 109-131**.

Zettner, C. M., and Yoda, M. (2001). "The circular cylinder in simple shear at moderate Reynolds numbers: An experimental study." *Experiments in Fluids*, 30(3), 346-353.

Zovatto, L., and Pedrizzetti, G. (2001). "Flow about a circular cylinder between parallel walls." ***Journal of Fluid Mechanics*, 440, 1-25**.